Regional dynamics of Calanus in the Norwegian Sea in response to ocean climate in 1997

Dag Slagstad, Kurt Tande, Webjorn Melle, Bjsrnar Ellertsen, Francois Carlotti

International Council for
the Exploration of the Sea

C M 2000/M:20
Plankton Committee

Regional dynamics of *Calanus* in the Norwegian Sea in response to ocean climate in 1997,

by

Dag Slagstad[1], Kurt Tande[2], Webjørn Melle[3], Bjørnar Ellertsen[3], François Carlotti[4]

[1]SINTEF Civil and Environmental Engineering, N-7465 Trondheim, Norway, [Dag.Slagstad@civil.sintef.no].
[2]University of Tromsø, N-9037 Tromsø, Norway [email: kurtt@nfh.uit.no].
[3]Institue of Marine Research, Bergen, Norway [email: webjoern.melle@imr.no];
[4]C.N.R.S. / Universite Bordeaux 1 Laboratoire d'Oceanographie Biologique, UMR 5805, 2, rue du Professeur Jolyet 33 120 Arcachon, France [email: carlotti@biocean.u-bordeaux.fr]

A coupled 3D hydrodynamic and ecological model has been set up for the Norwegian Sea (i.e. SINMOD). The hydrodynamic model uses the z-coordinates in the vertical direction. The horizontal grid point distance is 6.67 km and covers the northern North Sea, Mid Norwegian Shelf, Lofoten Basin, Faroes Shelf. The western limit is just at the eastern boarder of the Icelandic Shelf. The open boundaries are taken from a regional model using 20 km grid resolution. The models have been forced with atmospheric input from 6 hourly wind and pressure fields. The ecological model has eight state variables in addition to a structured model of *Calanus finmarchicus*. The state variables are nitrate, ammonium, silicate, diatoms, flagellates, microzooplankton, slow and fast sinking detritus. The *Calanus* model uses developmental structure for the nauplii and weight structure for the copepodites. Data from Station M (66°N, 2°E) has been used to adjust the mortality rates of *Calanus*. 10% of the CV's are allowed to develop into females and start a new generation and the remaining 90% is transferred into an overwintering stage having a depth distribution between 500 and 1500m. The overwintering stock of *Calanus* at Station M below 600m was taken as an initial distribution for the whole model domain (north of the Scotland-Iceland ridge). The model simulates the pattern of phytoplankton growth, which is in accordance with observational data from several cruises in the region during the year of *Calanus*. An early start (March/April) in the Coastal Norwegian waters and at the front between the coastal water and the Atlantic waters was found. The spring bloom starts gradually later West and North in the Norwegian Sea. The earliest spawning took place near the shelf break off Norway where ascending *Calanus* met the spring bloom in surface waters. At Station M the timing of the spring bloom and the successive copepodite stages are simulated correctly. The simulated second generation is two weeks earlier than observed in field data. However, there is a large heterogeneity around this position in the Norwegian Sea on the southwestern slope of the Vsring Plateau. Coastal water and perhaps water from the East Iceland Current may 'change the property (vertical mixing and nutrient supply) and the history of *the Calanus* stock entering this geographical region. Two generations *are* of *Calanus* simulated in the southeastern part of the Norwegian Sea. Along the shelf break the second generation is advected as far north as the entrance to the Barents Sea. In the Northern North Sea the temperature and the supply of food is sufficient for the model to produce three generations.

Introduction

Calanus finmarchicus is probably the most important zooplankton species as food for early life stages of most commercial fish species in the North East Atlantic. It occurs from the northeastern part of North America past the south-eastern edge of Greenland, as far south as through the English Channel into the North Sea, as far north as up to Svalbard and as far east as the Barents Sea. *Calanus* is usually in a diapause during the winter months and spend months in deep water, usually below 600 m, if such depth exists. This has the effect that the shelf areas will export *Calanus* during the decent phase of the ontogenetic migration (Slagstad and Tande 1996). In spring and summer there will be a net import from the oceanic regions.

The Generation pattern of *Calanus* has been much debated lately, and two or three generations has been suggested in the North Sea. In the paper we will use apply coupled hydrodynamic and ecological models to study the population dynamics of *Calanus* in the Norwegian Sea. The input is the meteorological forcing for the year 1997. On the other open end of the model, the mortality of *Calanus*, time and stage specific death rates are specified.

During the year 1997 there was an intensive sampling program within the Norwegian Sea. Especially, at the station M (66°N, 2°E) high-resolution time series of phytoplankton and *Calanus* were obtained. The spatial cover was less intensive and in order to get a spatial picture of ***the*** dynamics of *Calanus* in the Norwegian Sea, a numerical model that utilise some of the data obtained in the sampling program.

Model description

Hydrodynamic model

The hydrodynamic model is based on the primitive Navier-Stokes equations solved by a finite difference scheme. The model uses the z-coordinates in the vertical direction (i.e. each model level has a fixed thickness except for the surface level and the one close to the bottom). A detailed model description is found in (Stole-Hansen and Slagstad 1991; Moseidjord et al. 1999). The model domain covers an area of 2280x1200 km^2 which includes the northern North Sea, mid Norwegian shelf and most of the Norwegian Sea (Fig. 1). The horizontal grid point distance is 6.67 km and there are 21 vertical levels. The thickness of the levels from the surface is: 1 Om, 6x5m, 1 Om, 2x25m, 2x50m, 3 * 1 00m, 200m, 300m, 500m, 3 * 1 000m. The open boundaries for the nested model is generated by a regional model covering the Norwegian Sea, Barents Sea, and the Greenland Sea. The coupling between the models is performed by a flow relaxation scheme (Martinsen and Engedahl 1987). The horizontal grid point distance is 20 km and the vertical resolution is the same as for the nested model. On the open boundaries, the current velocities are specified, and temperature and salinity are taken from the monthly Levitus' (1982) database (Slagstad et al. 1999).

Atmospheric forcing is the same for both models. Wind and air pressure input is taken from the Norwegian Meteorological Institute's hindcast data archive (Eide et al. 1985) for the year 1997. The heat flux is calculated from air temperature, humidity, cloud cover which is interpolated from available meteorological stations within the model domain and the

theoretical height of the sun. Initial values of temperature and salinity were taken from the Levitus' database (Levitus 1982). Freshwater input is calculated from average seasonal run-off (Tolland 1974). Advection of any scalar property c is performed by the advection-diffusion equation

$$\frac{\partial c}{\partial t} + \mathbf{Adv(c)} + \mathbf{Diff(c)} = G$$

where G is the local rate of change of a constituent (e.g. temperature, salinity or a biological state variable). The two operators, Adv and Diff represent the advection and the diffusion terms, respectively, which are defined as:

$$\mathbf{Adv(c)} = \frac{\partial}{\partial x}(uc) + \frac{\partial}{\partial y}(vc) + \frac{\partial}{\partial z}(w + w_b)c$$

$$\mathbf{Diff(c)} = -\frac{\partial}{\partial z} K_v \frac{\partial c}{\partial z}$$

where t is time, x, y, z are the three spatial coordinates, u, v and w are the current speed in x, y, z directions, respectively; K_v is the vertical eddy diffusion coefficient. For later use we define the combined advection-diffusion term AD = Adv + Diff. The vertical eddy diffusion is calculated from the Richardsons number and a simplified surface wave model (Slagstad and Wassmann 1996). The numerical advection method for solving Eq.(2) is a so-called TVD (total variation diminishing) scheme (Yang and Przekwas 1992. This scheme has a very low numerical diffusion.

Ecological model

The model structure chosen here is based on the field investigations performed outside Northern Norway 1994 (Andreassen et al. 1999, Ratkova et al. 1999, Wassmann et al. 1999) and data from Station M in the Norwegian Sea (Melle and Ellertsen, TASC final report). The ecosystem model assumes that nitrogen and silicate are the potential limiting nutrients in the Norwegian Sea and consist of eight state variables (Fig. 2.). These are: nitrate (NO_3), ammonium (Na), silicate (Si), diatoms (Di), flagellates (F), microzooplankton (Mi), fast sinking detritus (Df), slow sinking detritus (Ds) and *Calanus finmarchicus* (Cf).

The Calanus model.

Structured models of a population need to select one or more properties, which characterize population in on way or another, depending on the purpose with the model. A population structure of a *Calanus* population is usually based on stage distribution. However, weight structure may also be used and this is often more convenient in models where energy balances often are important features. A structured population may be govern by the equation

$$(4) \quad \frac{\partial C_f}{at} + g_w \frac{dC_f}{dw} + g_d \frac{\partial C}{\partial d} = birth - mortality$$

where $C_f(w,d)$ is the concentration of a weight/developmental class of *Calanus*, g_w is the growth rate, w is weight, d is developmental level, g_d is rate of development (see Sinko 1969; Slagstad 198 1; Tande and Slagstad 1992; Giske et al. 1997 for further details). In order to reduce the computational work in a 3D model, only one property can be applied for representation of population structure. For nauplii, developmental stage is chosen and weight is assumed to represent the important features of the copepodites. In order to mimic important events in a copepods lifecycle (diapause as stage V, spawning etc.) a fixed relationship between the weight and stage of development is assumed (Tande and Slagstad 1992). The population equation (Eq. 4) is integrated by a 2.order method in time and property space.

The eggs and nauplii developmental axis is divided into 9 grid points and the copepodites into 29 grid points. In addition, there are a separate overwintering compartment recruited from CV animals going into diapause. This sums up to 39 compartments in addition to the 8 non-*Calanus* state variables. Each of these variables has to be advected with an appropriate vertical distribution in a 3D physical domain.

Rates of ingestion, respiration egestion are based on the results of various (e.g. Carlotti and Radach 1996). Nauplii start to feed as stage N5. We assume here that they feed on diatoms, only. Their lower feeding threshold is 20 $\mu g\ C\ l^{-1}$. The feeding depends linearly on the diatom concentration, reaching optimal concentration at 40 $\mu g\ C\ l^{-1}$. The non-feeding stages of nauplii have a developmental rate depending of temperature. The feeding stages slow down their developmental rate proportional to their gap between the optimal and the actual concentration of diatoms. The nauplii mortality rate is set to . 1 d^{-1} for the non-feeding stages. The feeding stages have a mortality rate of .15 d^{-1} when food is at or above optimal concentration, increasing linearly to .9 d^{-1} at the feeding threshold.

The copepodite stages were allowed to graze on both diatoms and microzooplankton, following a functional relationship described by Carlotti and Radach (1996). Maximum grazing rate was set to $W^{0.7}\ d^{-1}$. A linear functional relationship between available food and grazing were used. On the other hand, if the maximum grazing rate at a given temperature (G^{Mi}_{max}) cannot be sustained, the additional food is taken from diatoms. A linear functional relationship is used (see Table 2), starting from a lower feeding threshold (C^{Mi}_{Thresh}) and levels out at the critical concentration (C^{Mi}_{Crit}). Grazing on diatoms started at a lower threshold value of 40 $\mu g\ C\ l^{-1}$ and a optimal concentration of 100 $\mu g\ C\ l^{-1}$ was set, whereas the corresponding grazing parameters for microzooplankton were 7 $\mu g\ C\ l^{-1}$ and 50 $\mu g\ C\ l^{-1}$. The assimilation efficiency (a_{Cf}) was equal to 0.7 and the excretion rate (E_{cf}) was 10% of the grazing rate + 1% of the mesozooplankton biomass per day.

We assume that 10% of the CV continue to CVI and the others enters the diapause which mean that the try to enter the water column between 500 and 1500 m, if available. The new females are assumed to develop their gonads for 14 days before spawning.

Mortality is a rather tricky and important parameter to estimate in population model of this

type. Here, we have used the high resolution time series from Station M. A 1D model taking temperature and vertical mixing coefficients from the 3D model at the position of Station M simulated the population dynamics at this station. No advection was used. The mortality rates where then adjusted in order to fit the data (Fig. 3). The values found were 0.055 d^{-1} CI-CIII and 0.025 d^{-1} for CIV and CV. When animals went into diapause, the mortality rate was 0.001 d^{-1}. The mortality rate is not dependent on temperature or geographical position. This has the effect that if food is not limiting growth, the number of animals entering diapause will increase with increasing temperature.

The basic unit used in the model is mmol N m^{-3}. When conversion to carbon is needed, the Redfield ratio (Redfield al. 1963) is applied. An initial (winter value) concentration of nitrate was specified to 10 mmol m^{-3}.

The phytoplankton growth is a function of light, nutrients and temperature and will vary with solar elevation (i.e. the season, latitude and the time of the day) and position in the water column. A relationship between the solar elevation and photosynthetic available h-radiance (PAR) has been established by using a model of Bird (1984). The attenuation coefficient of light in the water column is calculated from an equation given in Parsons et al (1983) using the value for "the clearest oceanic water" and the chlorophyll concentration.

Using this operator as defined by equations 1-3, we can write the model equations as shown in Table 1.

Nutrient limitation on growth rate of diatoms and flagellates are calculated by a Michaelis-Menten equations. Nitrogen to support primary production is supplied from two sources, nitrate and ammonium and we assume that the limitation is the total nitrogen available (Fasham et al. 1990). The following expression is used for nitrogen limitation

$$(5) \quad G_N = \frac{No3}{k_N + No3} e^{-\psi Na} + \frac{Na}{k_N + N}$$

where k_N is the half saturation constant for uptake of nitrate and ammonium, ψ is a parameter determining the suppression of nitrate uptake in presence of ammonium. For diatoms, the nutrient limitation is the minimum of nitrogen, silicate or light limitation.

Loss of diatoms due to sedimentation of resting spores and aggregates are assumed caused by nutrient depletion. These, in nature, complex process is described by a formula given in Wassmann and Slagstad (1993) which transform diatoms into the compartment of fast sinking detritus

(6) $$S = (d_{mn} + (d_{mx} - d_{mn}))e^{-\min\{G_N^{Di}, G_{Si}^{Di}\}/d_g}$$

where S is the specific rate of conversion from diatoms to fast sinking detritus, d_{mn}, d_{mx} and d_g are parameters given in Table 2. A constant specific rate of dead diatoms and flagellates (often associated with respiration) are turned into slow sinking detritus.

The functional relationship of the photosynthetic active radiation (I_z) and the specific photosynthetic rate (f_I) is described by the following formula (PAR)

(7) $$f_I = 1 - e^{-\alpha^B I_z / P_m^B}$$

where α^B is the chlorophyll a-normalized photosynthetic efficiency and P_m^B is the chlorophyll a-normalized maximum gross photosynthetic rate (see also Jassby and Platt 1976; Sakshaug and Slagstad 1991).

No information is available for microzooplankton in the Norwegian Sea. Using information and experience from other areas we have reasons to believe that microzooplankton also is important in this region. Here we will take literature values and for grazing and growth of this functional group. The microzooplankton group consists of several species, which vary in biomass during the season (Ratkova et al. 1999, Verity et al. 1999). Microzooplankton is usually assumed to feed on flagellates (Hansen et al. 1993), but observations on diatom grazing have also been observed (Nejestgaard 1994). Here we assume that microzooplankton feed on flagellates.

Detritus is divided into a slow and a fast sinking component. The slow sinking component encompass non-assimilated material, dead bodies from microzooplankton and dead diatoms and flagellate cells, whereas the fast sinking component is made up by fecal pellets and dead bodies from mesozooplankton and sedimenting diatom cells (resting spores, aggregates, etc.). The fast sinking component has a sinking rate of 50 m d^{-1} and degradation rate of 0.33 d^{-1}, whereas the slow sinking component has a sinking rate of 1 m d^{-1} and a degradation rate of 0.05 d^{-1} (see Table 1 for model equations).

initial conditions

The initial nitrate concentration was 12 μmol l^{-1} in the oceanic waters (salinity $\geq$ 35.0) decreasing linearly with salinity to 8 at in coastal water (salinity 32.0). The silicate concentration was taken to be half of the concentration of nitrate. The overwintering number of females was taken from the Station M data, approximately 20000 m^{-2}. This concentration was the same for the whole model domain for depths greater than 600m and north of the Wyville-Thomson Ridge. Although higher numbers have been found in the Faroes-Shetland Channel, the Station M value has been applied in the simulation presented in this report.

Results

After a spin up period of half a year using atmospheric input data for 1996 and 1997, daily average flow fields were saved on disk for later use by the ecological model. The flow field was inspected and found to represent the major currents in the area. The Norwegian Sea Deep water outflow was 1.2 Sv, which is close to the observations. The low diffusive advection scheme combined with relative high grid resolution created several sharp frontal structures. On the eastern side, between the coast water and Atlantic waters and the western side between the East Iceland Current and the Atlantic waters.

Very few time series of biological state variables exist from the Norwegian Sea. At the weather ship, Station M (66 °N, 2 ° E), time series are available for phytoplankton, nutrients and *Calanus*. During 1997, the EU-funded project TASC, initiated an intensive sampling program at Station M and other sits in the North East Atlantic. We will compare model results from with this data set.

The simulation starts at March 1 with a flagellate concentration just below the assumed threshold for the microzooplankton. In the deep mixed water column, there is a slow increase in the flagellate biomass (Fig. 4C). The microzooplankton concentration increases slowly and reaches 7 $\mu g\ C\ l^{-1}$ around March 20. *Calanus* grazing starts and eggs which develops into the first naupliar feeding stage. Since we assume that diatoms must be available for the nauplii to develop, no further development is seen. In late April, the concentration of diatoms is sufficient for the nauplii to develop into copepodite. This pattern was also observed during the spring 1997 (Niehoff et al. 1999). The diatom bloom that follows has its peak in the second half of May. The successive copepodite stages follow in May -June. Stage CIII is at its maximum when the diatom bloom has the highest concentration. The diatom bloom is terminated by shortage of silicate.

The first sign of the second generation was already found in late June, as nauplii become apparent. However, due to lack of diatoms further development into the copepodite stages did not take place. In mid July, which is 14 days earlier than in the observed data the CI of the second generation was seen. When simulating this dynamics without advection (only vertical mixing taken from the 3D hydrodynamic model), the second generation was actually found in early August. This indicates that the early arrival of the second generation is due to advection of nearby patches of water where the copepodite development is more advanced.

The spatial distribution of diatoms is shown for selected dates in Fig. 5. The production starts first in the near coastal regions and the North Sea as found in Rey (198 1 a and 198 1 b) . Outside More, there is a bifurcation of the Norwegian Coastal current. The main branch follows close to the coast whereas a smaller branch joins the Norwegian Atlantic Current at the shelf break. This brings some low salinity water to the shelf break and reduces the depth of vertical mixing. The result is early primary production. In mid May, the inner mid Norwegian shelf has already a very low concentration of diatoms at the surface. The bloom progress from the coast towards western part of Norwegian Sea. In early July the surface concentration of diatoms is almost zero, except for a small are outside Møre were wind induced upwelling take place

Since we started this simulation without overwintering females on the shelf, there are only a few animas on the shelf that can utilise the early start of primary production. At the shelf

break there is an early production start and females from the oceanic overwintering stock which. The result is early spawning and early copepodite stages are seen here already in mid April.

Copepodites CI are first seen in mid April along the shelf break where the early growth of phytoplankton and the ascending females meet (Fig.6). The phytoplankton production in the Norwegian Coastal Current could have sustained *an* earlier *start* of *Calanus* production, but the females must be supplied from other overwintering sources (Norwegian Trench, fjords or deep trenches on the shelf) than the oceanic stock. It is a clear pattern of gradually delayed CI appearance toward the west and north. This is even more pronounced for the CIV (Fig 7.).

Although the North Sea is just on the edge of the model domain and the lateral boundary condition here is zero for all copepodite stages, this northern North Sea appears to be very productive. The overwintering generation is advected in to the area along the western slope of The Norwegian Trench. High summer temperatures gives a short generation time and we observe production of 3 generations. The mortality rates that were adapted from the Station M are probably far to low for this region of the model domain. The simulations also show that the deep distribution of animals in the Norwegian Trench also give some export of overwintering CV into the Norwegian Sea (not shown). As seen on Fig 7, the lower left panel, the 3.generation in the North Sea an south West Coast of Norway, coincide in time with the 2. Generation out in the Norwegian Sea

The model produced up to 3 generations in the south where the temperature was highest. We don't know the mechanism why CV chose to go for a new generation or start overwintering. It may well be that animals in the south have only one or two generations, but the model indicate that 3 generations are possible from a temperature-developmental rate and food supply point of view.

ACKNOWLEDGEMENT

The computational needs for this model study have been demanding. One simulation run took 7 days of computation. Without support from the High Performance Computing Program at the University of Tromss this work would not have been possible. This paper is a contribution to TASC and funded by EU Contract No MAS3-CT95-0039.

REFERENCES

Andreassen IJ, Wassmann P, Ratkova TN. 1999. Seasonal variation of vertical flux of phytoplankton and biogenic matter at Nordvestbanken, north Norwegian shelf in 1994. - *Sarsia* 84:227-238.

Bird RE. 1983. A simple, solar spectral model for direct-normal and diffuse horizontal irradiance. - *Solar Energy 32:* 461-471.

Carlotti F, Radach G. 1996. Seasonal dynamics of phytoplankton and *Calanus finmarchicus* in the North Sea as revealed by a coupled 1-D model.. *Limnology and Oceanography* 41, 522-539.

Eide LI, Reiestad M, Guddal J. 1985.Database av beregnede vind og bølgeparametre for Nordsjsen, Norskehavet og Barentshavet, hver 6. time for årene 1955-81. The *Nor-*

wegian Meteorological Institute, Oslo/Bergen, 38 pp.

Fasham MJR, Ducklow HW, McKelvie SM. 1990. A nitrogen-based model of plankton dynamics in the oceanic mixed layer. - ***Journal*** *of* ***Marine Research 48:*** 591-639.

Giske J, Skjoldal HR, Slagstad D. 1998. Ecological modelling for fisheries. In T. Rødseth: Models for Multispecies Management. Pp. 1 l-68. Physica-Verlag Heidelberg.

Halvorsen E. 1997. Physical and biological factors influencing the seasonal variation in distribution of zooplankton across the shelf at Nordvestbanken, Northern Norway. Cand. Scient Thesis, University of Tromsø.

Halvorsen E, Tande K. 1999. Physical and biological factors influencing the seasonal variation in distribution of zooplankton across the shelf at Nordvestbanken, Northern Norway. - ***Sarsia*** 84:279-292.

Hansen FC, Reckermann M, Klein Breteler WCM, Riegman R.1993. ***Phaeocystis*** blooming enhanced by copepod predation on protozoa: evidence from incubation experiments. - ***Marine*** *Ecology* ***Progress Series*** 102: 5 l-57

Hopkins TS. 1991. The GIN Sea - A synthesis of its physical oceanography and literature review 1072-1985. Earth-Science Reviews 30: 175-318.

Irigoien X, Head R, Klenke U, Meyer-Harms B, Harbour D, Niehoff B, Hirche H-J, Harris R. 1999. . A high frequency time series at Weathership M, Norwegian Sea, during the 1997 spring bloom: feeding of adult female *Calanus finmarchicus*.

Johansen V. 1997. Life Cycle Strategy and Advection of *Calanus* ***Finmarchicus*** in the Norwegian Sea. Diploma thesis. Norwegian University of Technology and Science (NTNU), Trondheim

Levitus S., 1982. Climatological atlas of the word ocean. NOAA Prof. pap. 13, 173p.

Neijstgaard JC, Witte JH, der Wal Pv, Jacobsen A. 1994. Copepod grazing during a mesocosm study of ***an*** *Emiliania huxleyi* (Prymnesiophyceae) bloom. - ***Sarsia 79: 239-377***

Martinsen E, Engedahl H.1987. Implementation and testing of a lateral boundary scheme as an open boundary condition in a barotropic model. Coastal Engineering 11: 603-627.

Niehoff B, Klenke U, Hirche H-J, Irigoien X, Head R, Harris R. 1999. A high frequency time series at Weathership M, Norwegian Sea, during the 1997 spring bloom: the reproductive biology of *Calanus finmarchicus*. Marine Ecology Progress Series 176: 81-92.

McLaren IA 1978. Generation lengths of some temperate marine copepods: estimation, production and implications, J. Fish Res. Bd Can. 345: 1330-1342.

Miller C, Tande K. 1993. Stage duration estimation for *Calanus* population, a modelling study. Mar. Ecol. Prog. Ser. 102: 15-34.

Moseidjord H, Svendsen H, Slagstad D. 1999. Sensitivity studies of circulation and ocean-shelf exchange off northern Norway. - Sarsia 84: 191-l 98.

Parsons TR, Takahashi M, Hargrave B. 1983. Biological Oceanograpic Processes. Oxford,

Pergamon Press, 330pp.

Ratkova TN, Wassmatm P, Verity PG, Andreassen IJ. 1999. Abundance and biomass of pico-,nano- and microzooplankton along a transect across Nordvestbank, north Norwegian shelf, in ***1994.*** *-Sarsia* 84:2 13-225.

Redfield AC, Ketchum BH, Richards FA. 1963. The influence of organisms on the composition of sea-water. In The Sea, ed. M.N. Hill, Vol. 2, pp. 26-77. John Wiley, New York.

Rey F. 198 1 a. Primary production estimates in the Norwegian Coastal Current between 62°N and 72°N. - Pp. 640-648 in: Sætre, R. and M. Mork (eds). The Norwegian Coastal Current. University of Bergen.

Rey F. 198 1 b. The development of the spring phytoplankton outburst at selected sites off the Norwegian coast. - Pp. 649-680 in: Sætre, R. and M. Mork (eds). The Norwegian Coastal Current. University of Bergen.

Sakshaug E, Slagstad D. 199 1. Light and productivity of phytoplankton in polar marine ecosystems: A physiological view. Polar Research 10: 69-85.

Sinko JW. 1969. A new mathematical model for describing the age-size structure of population of simple animals. Ph. D Thesis, University of Rochester. 137pp.

Slagstad D. 198 1. Modeling and simulation of physiology and population dynamics of copepods. Effects of physical and biological parameters. Modeling, Identification and Control 2: 119- 162.

Slagstad D, Tande KS (1996) The importance of seasonal vertical migration in the across shelf transport of *Calanus finmarchicus*. Ophelia 44: 189-205

Slagstad D, Tande K, Wassmann P. 1999. Modelled carbon fluxes as validated by field data on the North Norwegian shelf during the productive period in 1994. Sarsia 84: 303-317.

Slagstad D, Wassmann P. 1996. Climate change and carbon flux in the Barents Sea: 3-D simulations of ice-distribution, primary production and vertical export of particulate organic matter. Mem. Natl. Inst. Polar Res., Spec. Issue 5 1: 119-141.

Stole-Hansen K, Slagstad D. 1991. Simulation of currents, ice melting, and vertical mixing in the Barents Sea using a 3-D baroclinic model. Polar Research 10: 33-44.

Tande KS. 1991. *Calanus* in high latitude environments. ***Polar Research*** 10: 389-407.

Tollan A. 1974. River runoff in Norway. Pp 1 l-13 in: Skreslet, S. (ed). ***Influence of freshwater outflow on biological processes in fjords and coastal waters.*** Springer-Verlag, New York.

Verity PG, Andreassen IJ, Wassmann P, Ratkova PTN, Nordby E. 1999. Seasonal patterns in composition and biomass of autotrophic and heterotrophic nano- and microplankton communities on the north Norwegian shelf. –*Sarsia* 84:265-277.

Wassmann P, Slagstad D. 1993. Seasonal and annual dynamics of particulate carbon flux in the Barents Sea - A model approach. Polar Biology 13, 363-372.

Wassmann P, Andreassen IJ, Rey F. 1999. Seasonal variations of nutrients and suspended

biomass along and across a transect across the Nordvestbank, north Norwegian shelf, in *1994.* -*Sarsia 84:* 199-2 12.

Yang, HQ and Przekwas, AJ. 1992. Acomparative study of advanced shock-capturing schemes applied to Burgers' equation. Journal of Computational Physics. 102: 139-159.

Adlandsvik B, Eriksrød G. 1999. A hindcast simulation of currents in the Nordic Seas. Report from the TASC project.

FIGURE CAPTIONS

Figure 1 Model domain for the nested and the regional scale model setups. A filled circle shows position of Station M (66" N, 2" E).

Figure 2. Conceptual ecosystem model.

Figure 3. Time series data of CI-CIII (upper left panel), CIV-CV (lower left), depth integrated Chlorophyll biomass (upper right) from Station M.

Figure 4. Simulated time series from Station M. (A) vertical distribution of nitrate ($\mu mol\ l^{-1}$), (B) four day average of primary production ($gC\ m^{-2}\ d^{-1}$), (C) surface concentration of diatoms, flagellates and microzooplankton ($mgC\ m^{-3}$), (D) depth integrated grazing of *Calanus* on diatoms and microzooplankton ($gC\ m^{-2}\ d^{-1}$), (E) nauplii development (individual model grid points (9), and (F) stage distribution of the copepodites ($Nos\ m^{-2}$).

Figure 5. Simulated surface concentration of diatoms (mm01 N m^{-3}) at selected dates.

Figure 6. Simulated distribution of *Calanus* CI ($Nos\ m^{-2}$) at selected dates.

Figure 7. Simulated distribution of *Calanus* CIV ($Nos\ m^{-2}$) at selected dates.

Table Model Equations

(8) ∂Di AD(Di) Di[P_{Di}^{B}(T) min{f_I, G_N G_{Si}) S(No3, Si)] G_{Mi}

(9) ∂t AD(F) F[P_F^B(T) min{f_I, G_N} μ_F] G_{Mi}

10) $\partial No3$ AD(No3) = DiP_{Di}^{B}(T) min{f_I G_N G_{Si}} FP^B(T) min{f_I, G_N^F} ϕ

∂Na ∂t AD(Na) min{f_I, G_N, G_{Si}} FP_F^B min{f_I, G_N} ϕ_{Na} CfE$_{Cf}$ MiE$_{Mi}$ $_{Ds}$Ds Df Df

∂Mi $AD(Mi)$ $Mia_{Mi}\{G_i^{Di}$ $G_{Mi}^F\}$ $E_{Mi}(Di\ F)$ $_{Mi}$] $CfG_{Cf}^{Mi}(Di, Mi)$

∂Ds ∂t AD(Ds) Mi(1 a_{Mi}) × (G $_{Mi}$) μ_{Di}Di μ_FF $_{Ds}$Ds

∂Df ∂t AD(Df) = DiS(No3, a_C)Cf

Table 2 Parameters used in the biological model

Variable	Value	Units	Meaning
α^{B}_{Di}	0.02	mg C (mg Chl*a*)$^{-1}$ h^{-1} (mmol m^{-2} s^{-1})$^{-1}$	Chlorophyll *a*-normalized photosynthetic efficiency of diatoms
α^{B}_{F}	0.035	mg C (mg Chl*a*)$^{-1}$ h^{-1} (mmol m^{-2} s^{-1})$^{-1}$	Chlorophyll *a*-normalized photosynthetic efficiency of flagellates
P^{B}_{Di}	1.05	mg C (mg Chl*a*)$^{-1}$ h^{-1}	Chlorophyll *a*-normalized maximum gross photosynthetic rate of diatoms
P^{B}_{F}	2.0	mg C (mg Chl*a*)$^{-1}$ h^{-1}	Chlorophyll *a*-normalized maximum gross photosynthetic rate of flagellates
N_C		-	nitrogen to carbon ratio
Chl*a*_C_{Di}	0.03	-	Chl *a* : C ratio in the diatoms
Chl*a*_C_{F}	0.02	-	Chl *a* : C ratio in the flagellates
k_N	0.4	mmol m^{-3}	half-saturation constant for nitrate
μ_{Di}	0.05	d^{-1}	mortality rate of diatoms
μ_F	0.05	d^{-1}	mortality rate of flagellates
g^{Mi}_{max}	0.63	d^{-1}	maximum specific grazing rate of microzooplankton on flagellates at 0°C
C^{Mi}_{Thresh}	5	mg C m^{-3}	lower feeding threshold for microzooplankton feeding on flagellates
c^{Mi}_{Crit}	30	mg C m^{-3}	critical concentration for microzooplankton feeding on flagellates
μ_3			mortality rate of microzooplankton
a_{Mi}	0.7	-	Assimilation efficiency of microzooplankton
k_w	0.04	m^{-1}	Attenuation coefficient for pure sea water
a_{Cf}	0-7	-	Assimilation efficiency of mesozooplankton
ψ		(mmol N m^{-1})$^{-1}$	Parameter describing the inhibition effect on nitrate uptake by ammonium
dmn	0.004	h^{-1}	Parameter (Eg. 6)
dmx	0.02	h^{-1}	Parameter (Eq. 6)
a_{Cf}dg	0.1	-	Patameter (Eq. 6)

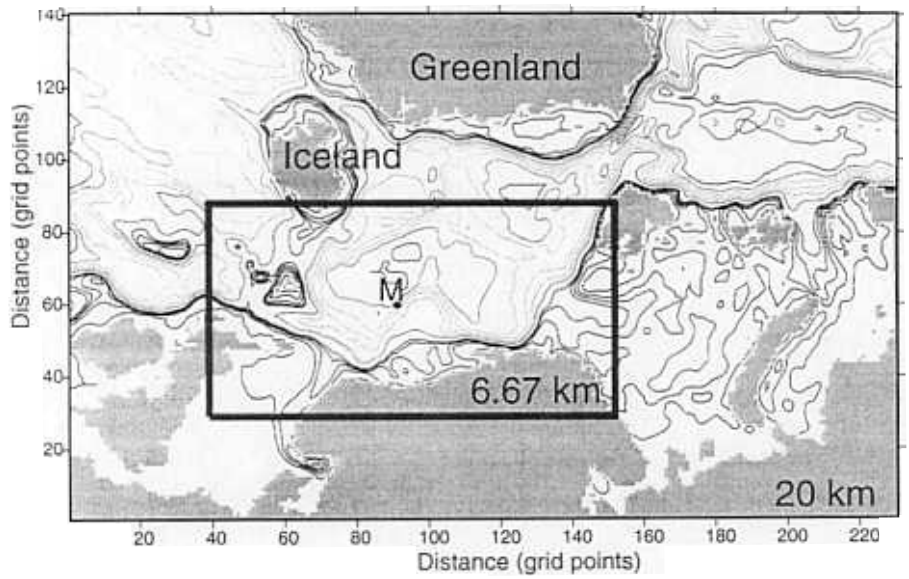
Greenland
Iceland
M
6.67 km
20 km
Distance (grid points)
Distance (grid points)
20
40
60
80
100
120
140
160
180
200
220

Fig

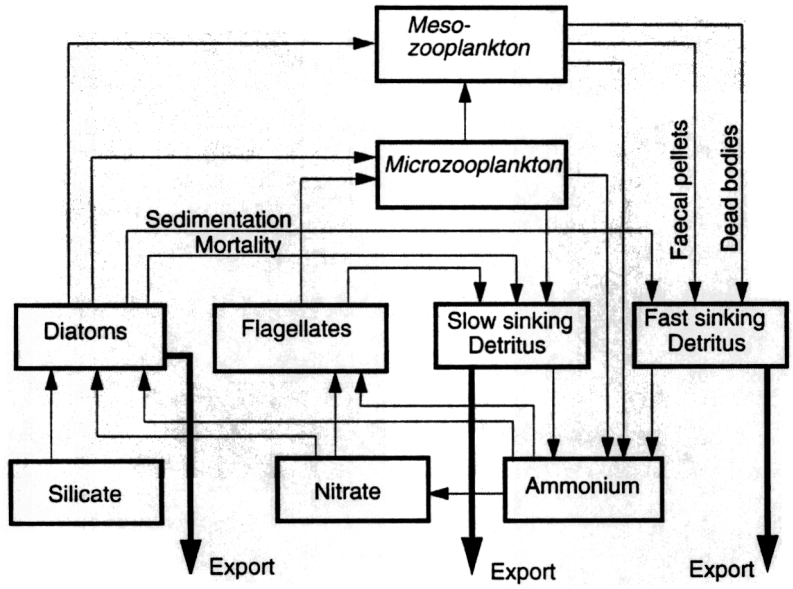
Meso-
zooplankton
Microzooplankton
Sedimentation
Mortality
Faecal pellets
Dead bodies
Diatoms
Flagellates
Slow sinking
Detritus
Fast sinking
Detritus
Silicate
Nitrate
Ammonium
Export
Export
Export

Fig 2

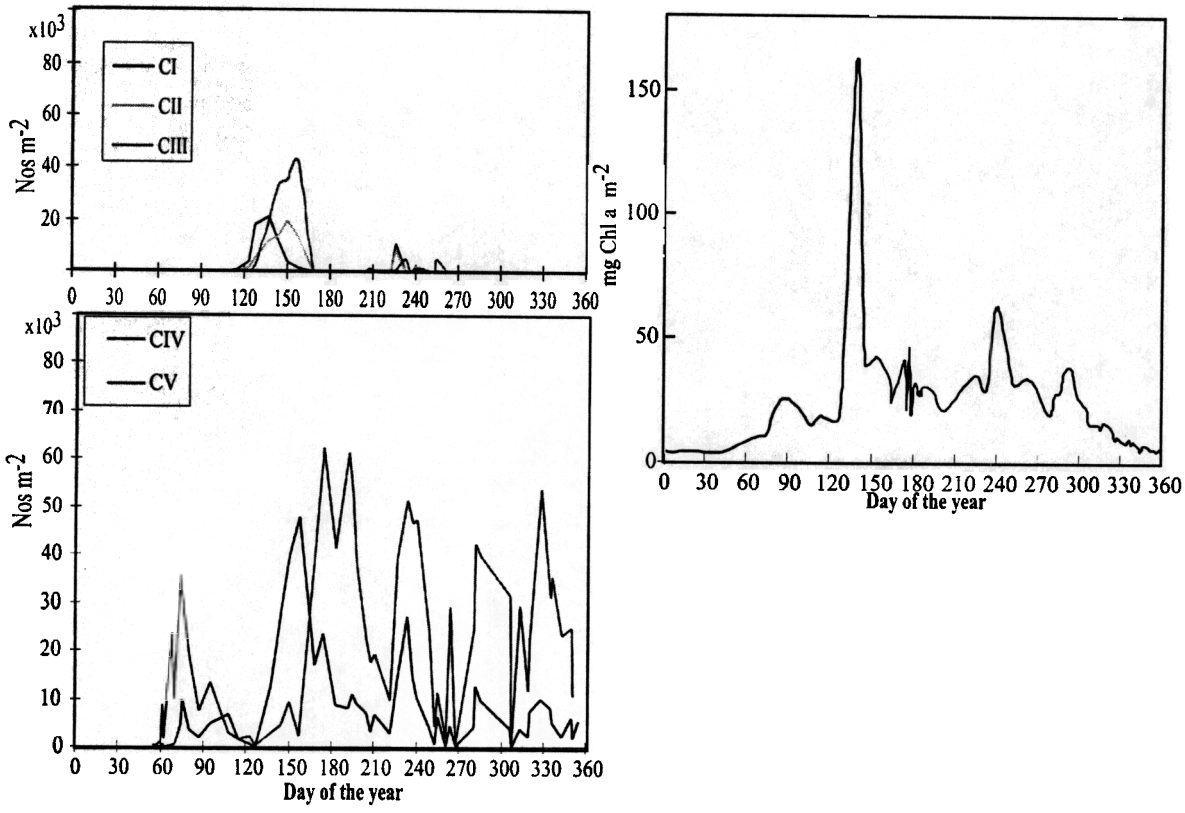
x10^3
Nos m^-2
CI
CII
CIII
CIV
CV
0 30 60 90 120 150 180 210 240 270 300 330 360
Day of the year
mg Chl a m^-2
0 50 100 150
Day of the year

Fig. 3

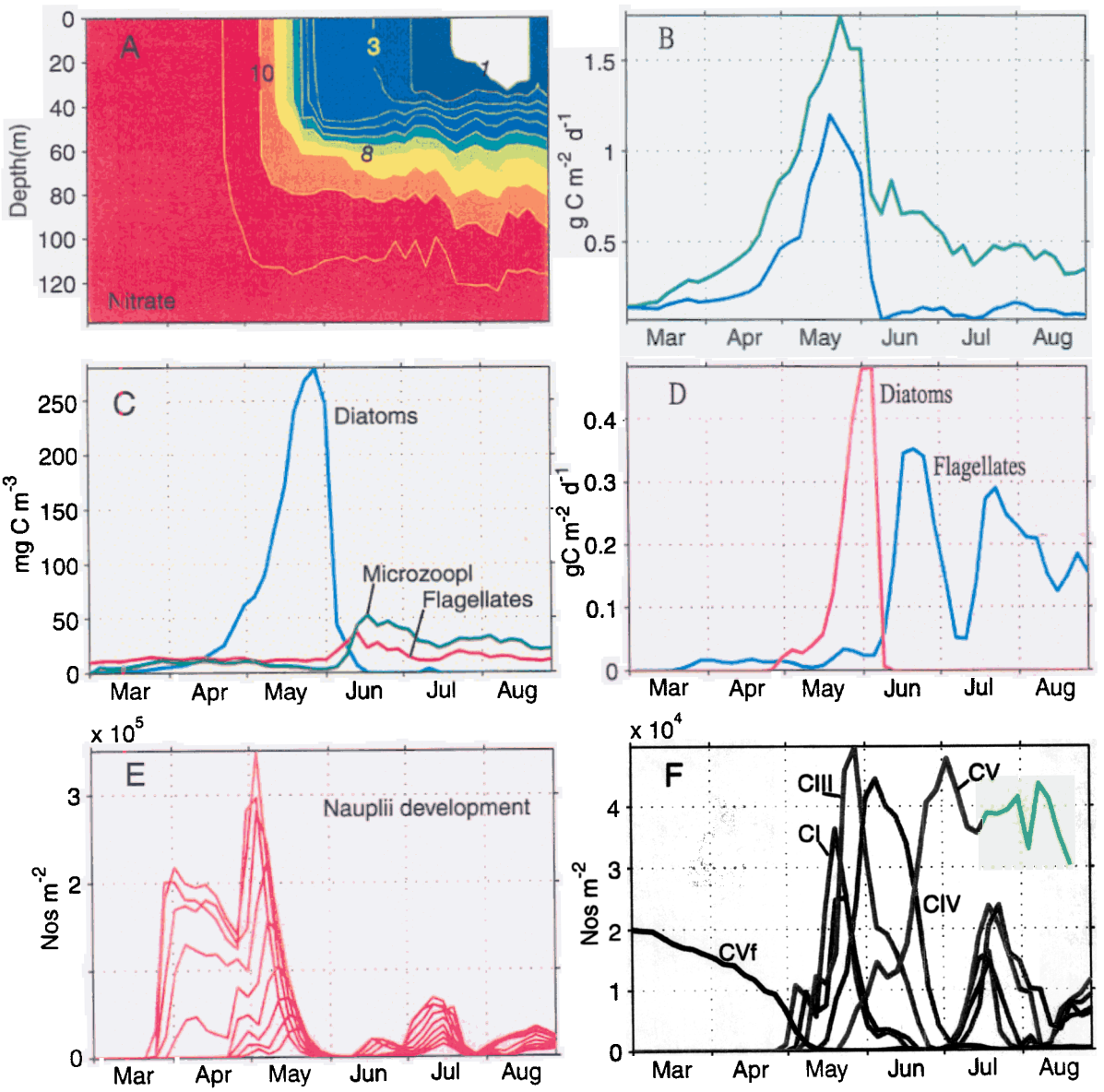
A
Depth(m)
0
20
40
60
80
100
120
Nitrate
10
3
8
B
g C m-2 d-1
1.5
1
0.5
Mar
Apr
May
Jun
Jul
Aug
C
mg C m-3
250
200
150
100
50
0
Diatoms
Microzoopl
Flagellates
D
gC m-2 d-1
0.4
0.3
0.2
0.1
0
Diatoms
Flagellates
E
x 10^5
Nos m-2
3
2
0
Nauplii development
F
x 10^4
Nos m-2
4
3
2
1
0
CIII
CI
CV
CIV
CVf

Fig. 4

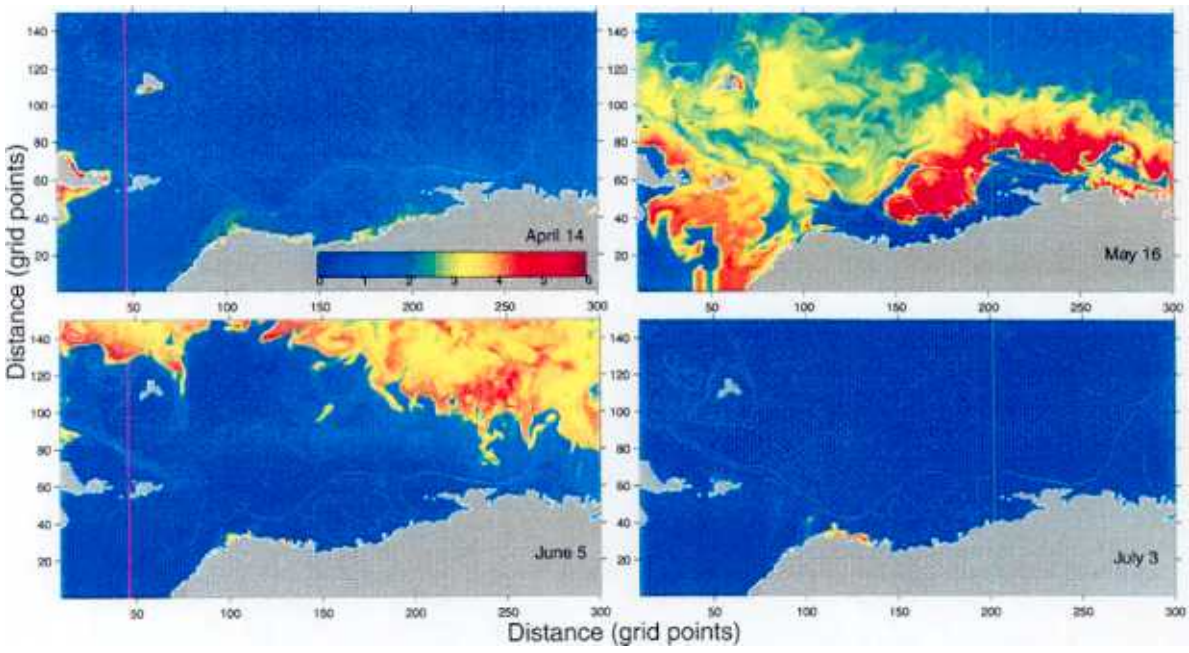
April 14
May 16
June 5
July 3
Distance (grid points)
Distance (grid points)

Fig. 5

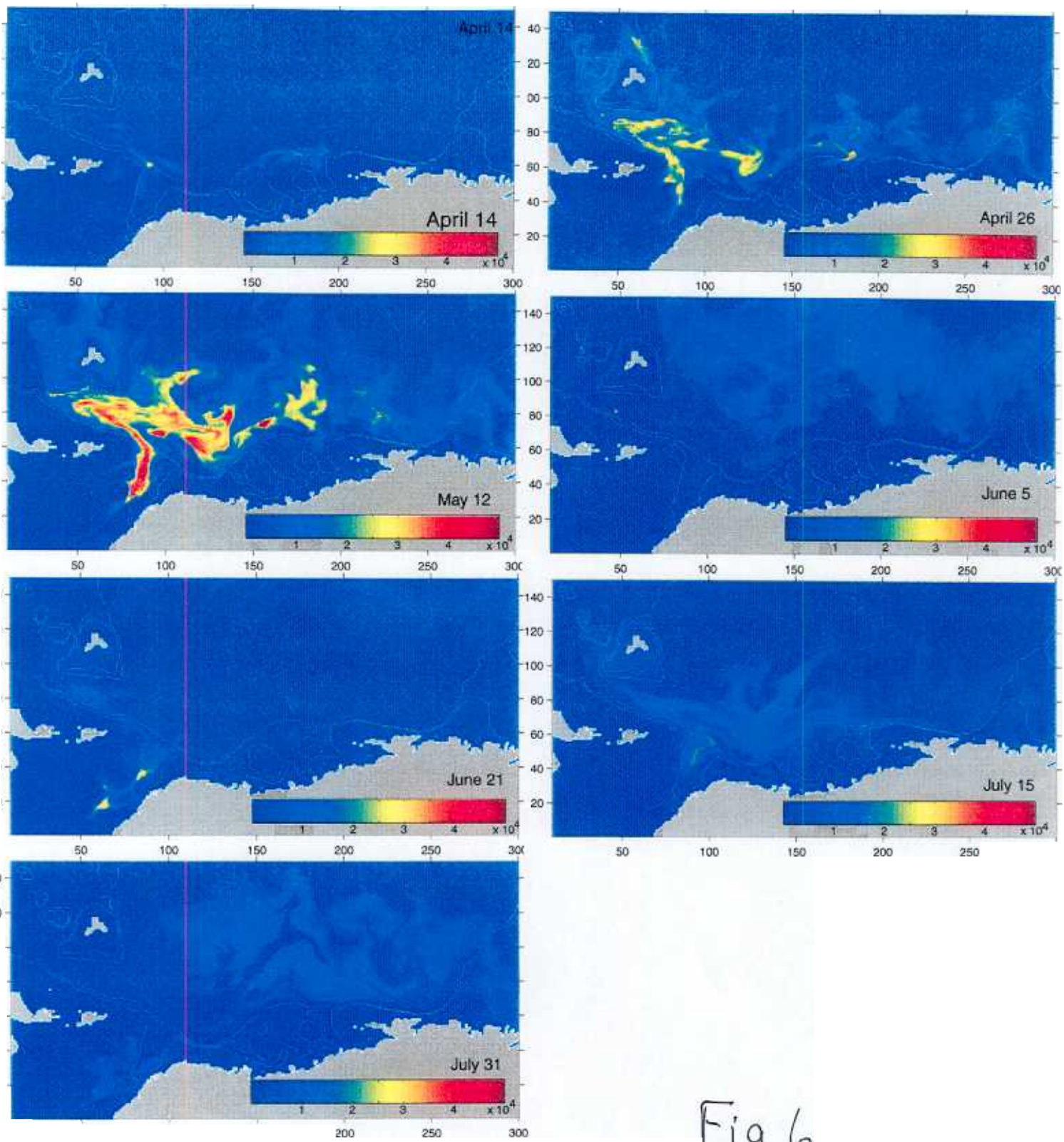

Fig 6

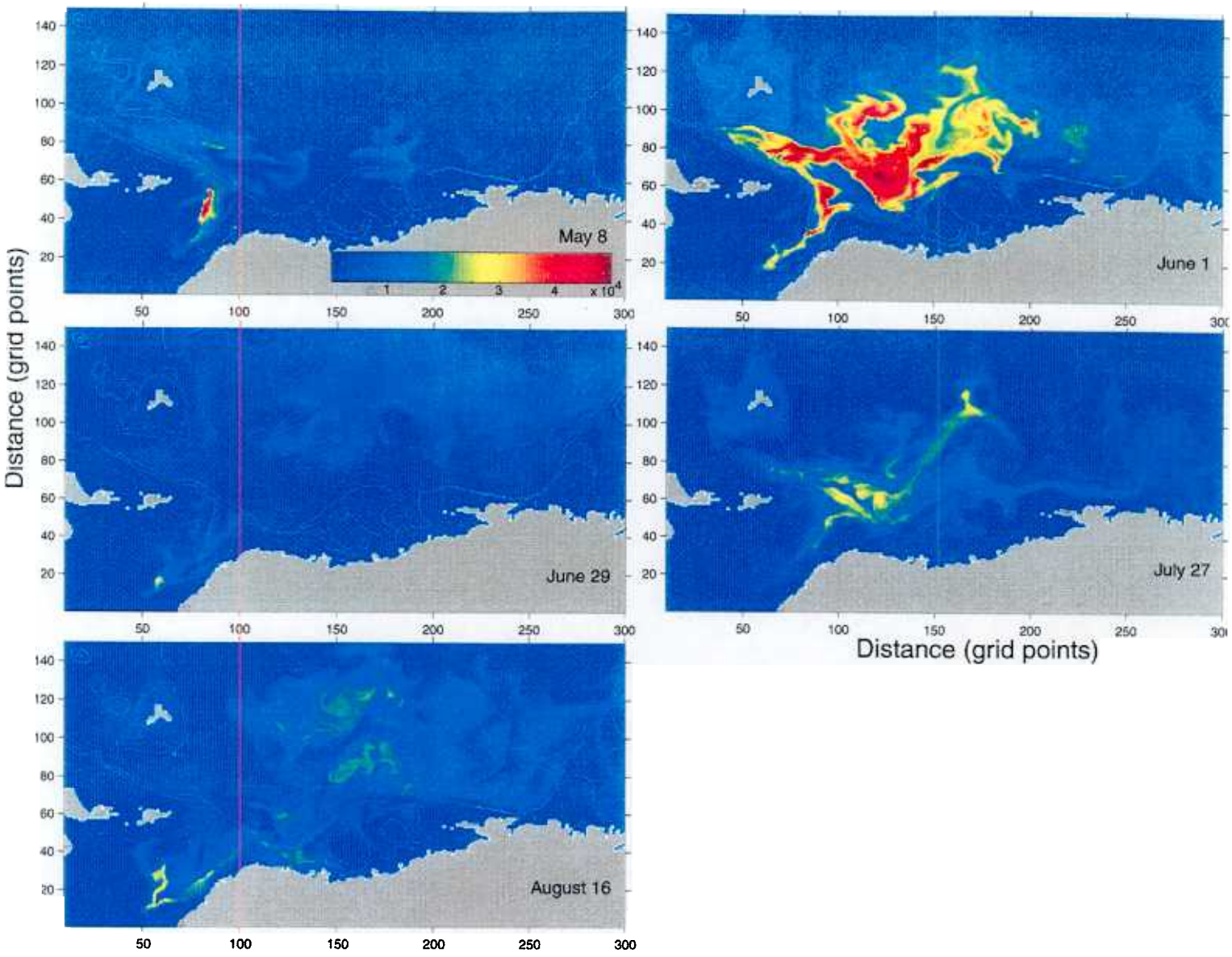
May 8
June 1
June 29
July 27
August 16
1
2
3
4
x 10^4
Distance (grid points)
Distance (grid points)

Fig 7